

# Characterisation of the Fermi surface and phase transitions of (BEDO-TTF)<sub>2</sub> ReO<sub>4</sub>·(H<sub>2</sub>O) by physical property measurements and electronic band structure calculations

S. Kahlich<sup>1</sup>, D. Schweitzer<sup>1</sup>, C. Rovira<sup>2,\*</sup>, J.A. Paradis<sup>2</sup>, M.-H. Whangbo<sup>2</sup>, I. Heinen<sup>3</sup>, H.J. Keller<sup>3</sup>, B. Nuber<sup>3</sup>, P. Bele<sup>4</sup>, H. Brunner<sup>4</sup>, R.P. Shibaeva<sup>5</sup>

<sup>1</sup> 3. Physikalisches Institut der Universität Stuttgart, Pfaffenwaldring 57, D-70550 Stuttgart, Germany

<sup>2</sup> Department of Chemistry, North Carolina State University, Raleigh, NC 27695-8204, USA

<sup>3</sup> Anorganisch Chemisches Institut der Universität Heidelberg, Im Neuenheimer Feld 270, D-69120 Heidelberg, Germany

<sup>4</sup> MPI für medizinische Forschung, AG: Molekulkristalle, Jahnstrasse 29, D-69120 Heidelberg, Germany

<sup>5</sup> Institute of Solid State Physics, Russian Academy of Sciences, 142432 Chernogolovka, Russian Federation

Received: 9 September 1993

**Abstract.** The electronic properties of the organic superconductor (BEDO-TTF)<sub>2</sub> ReO<sub>4</sub>·(H<sub>2</sub>O) were investigated by temperature dependent resistivity, ESR, Hall effect and magnetoresistance measurements. Shubnikov-de Haas (SdH) oscillations were observed in magnetic fields up to 24 T in the temperature range 0.5 K to 4.2 K. The electronic band structure of (BEDO-TTF)<sub>2</sub> ReO<sub>4</sub>·(H<sub>2</sub>O) was calculated by employing the extended Hückel tight binding method on the basis of its room temperature crystal structure. The two observed SdH frequencies of 75 T and 37 T correspond very well with two cross-sectional areas of the hole and electron Fermi surface pockets obtained from the tight binding calculation. From the temperature dependence of the SdH oscillation amplitudes, the cyclotron effective mass ( $m_c$ ) belonging to the larger and smaller pockets were found to be  $0.9 m_0$  and  $m_c = 1.15 m_0$  respectively. Measurements of the angular dependence of the SdH frequencies show no deviation from that expected for a cylindrical Fermi surface. In terms of our tight binding calculations and experimental measurements, probable causes for the 213 K and  $\sim 35$  K phase transitions are discussed. The calculations show that (BEDO-TTF)<sub>2</sub> ReO<sub>4</sub>·(H<sub>2</sub>O) is a two dimensional semimetal but possesses a hidden nesting. The latter is likely to cause an SDW instability leading to the  $\sim 35$  K transition. The resistivity drop associated with the 213 K transition is likely to be induced by an abrupt increase in the relaxation time. The excellent agreement between the calculated and experimentally observed Fermi surface implies that, with decreasing temperature below 35 K, (BEDO-TTF)<sub>2</sub> ReO<sub>4</sub>·(H<sub>2</sub>O) gradually gets out

of the SDW state and re-enters the “original” metallic state, in which it becomes superconducting below 2.4 K.

**PACS:** 71.25; 74.70.K

## Introduction

Since the first report of superconductivity in (TMTSF)<sub>2</sub>PF<sub>6</sub> [1], about 40 more organic superconductors have been discovered [2]. Most organic superconductors are radical salts of the organic donor BEDT-TTF (bis(ethylenedithio)tetrathiafulvalene). BEDO-TTF (bis(ethylenedioxy)tetrathiafulvalene) [3], an isostructural analogue of BEDT-TTF, led to a number of metallic salts as well [3–9], but only two salts, (BEDO-TTF)<sub>3</sub>Cu<sub>2</sub>(NCS)<sub>3</sub> [5] and (BEDO-TTF)<sub>2</sub>ReO<sub>4</sub>·(H<sub>2</sub>O) [8, 9], have so far been found to be superconductors.

(BEDO-TTF)<sub>2</sub>ReO<sub>4</sub>·(H<sub>2</sub>O) undergoes several interesting phase transitions [8–12]. The dc resistivity [8, 9] and thermopower [8] of (BEDO-TTF)<sub>2</sub>ReO<sub>4</sub>·(H<sub>2</sub>O) exhibit a metallic behavior down to 213 K, where a first order phase transition occurs [8–10] and the resistivity abruptly decreases by about a factor of two. In the temperature range between 213 K and about 35 K, the crystal again exhibits a metallic character, from  $\sim 35$  K to  $\sim 4$  K, the resistivity increases considerably and finally starts to decrease below  $\sim 3$  K to reach a superconducting state with an onset temperature of 2.4 K. In addition, thermopower measurements [8] suggest another phase transition at  $\sim 90$  K but also show a clear metallic behavior for the temperature range below 35 K. The occurrence of several phase transitions is interesting especially because (BEDO-TTF)<sub>2</sub>ReO<sub>4</sub>·(H<sub>2</sub>O) is a two dimensional (2D) metal according to the dc resistivity measurements [10] and preliminary measurements of Shubnikov de Haas (SdH) oscillations in magnetic fields below 7 T

---

Reported at the 13th General Conference of the Condensed Matter Division of the European Physical Society, Regensburg, March 1993

\* *Permanent address:* Departament de Química Física, Universitat de Barcelona, E-08028 Barcelona, Spain

[11]. The metal metal transition at 213 K can be suppressed by a pressure of about 19 kbar [9–11]. On the other hand, a relatively small pressure of 1 kbar is already sufficient to suppress the increase in resistivity below 35 K and sharpen the superconducting transition [10, 11].

Low dimensional metals are susceptible to charge density wave (CDW) or spin density (SDW) instabilities when their Fermi surfaces are nested [13, 14]. Several low dimensional metals exhibit CDW instabilities expected for one dimensional (1D) metals even though their individual Fermi surfaces possess a 2D metallic character. This puzzling phenomenon has been explained in terms of the hidden nesting concept [15], which refers to the fact that an electronic instability can arise from hidden 1D Fermi surfaces. The latter are found by combining the individual 2D Fermi surface together and neglecting the surface noncrossings. In understanding the CDW instabilities of the organic conducting salts (BEDT-TTF)<sub>2</sub>ReO<sub>4</sub>· [16] and (BEDT-TTF)<sub>4</sub>Pt(C<sub>2</sub>O<sub>4</sub>) [17], the hidden nesting concept has also been found essential [18]. Thus, it is important to probe whether or not the hidden nesting concept is also responsible for the increase of the resistivity below 35 K of the 2D metal (BEDO-TTF)<sub>2</sub>ReO<sub>4</sub>·(H<sub>2</sub>O).

In the present work, we investigated the Fermi surface of (BEDO-TTF)<sub>2</sub>ReO<sub>4</sub>·(H<sub>2</sub>O) by SdH measurements in magnetic fields up to 24 T in the temperature range 0.5 to 4.2 K and we calculated the electronic band structure by employing the extended Hückel tight binding (EHTB) method [19] on the basis of its room temperature crystal structure. Furthermore Hall effect – and ESR measurements were carried out to obtain more information of the probable causes for the metal metal phase transition at 213 K and the phase transition at ~35 K where a resistivity increase is observed.

## Experimental

BEDO-TTF was synthesised as described by Suzuki et al. [3]. Crystals of (BEDO-TTF)<sub>2</sub>ReO<sub>4</sub>·(H<sub>2</sub>O) were prepared by using the usual electrochemical preparation by taking KReO<sub>4</sub> as electrolyte salt together with 18-crown-6 ether in 1,1,2-trichloroethane (TCE). The crystal preparation was similar as described earlier for (BEDT-TTF)<sub>2</sub>Cu(NCS)<sub>2</sub> [20].

The resistivity measurements were carried out by the usual four point method. On all measured crystals four gold contacts were deposited by evaporation techniques and gold wires with gold paint connected to these contacts. SdH-measurements were done in the High Field Laboratory of the Max Planck Institut in Grenoble, in magnetic fields up to 24 T and in the temperature range 0.5 K–4.2 K. The crystals were mounted in a holder such that they could be tilted (during the experiment) around their *a*\*- and *c*-axis, the initial field orientation always being along the *b*-axis (normal to the *a*\*-*c*-plane of conduction) [8].

The Hall effect measurements were done in a fixed magnetic field of 6.8 T in the temperature range 1.3 K–

280 K. The gold contacts at the crystals were again deposited by evaporation techniques. The magnetic field orientation was along the *b*-axis. The current flow was parallel to the *c*-axis and the Hall-voltage  $U_H$  measured in *a*\*-direction.  $U_H$  was obtained from two independent measurements with the magnetic field direction turned by 180° with respect to each other.

The ESR investigations were performed with an X-band spectrometer (Bruker ESP 300) from 4.2 K to 300 K. A single ESR line was observed, as is typical for conduction electrons of a metal. The spin susceptibility was obtained by the usual way from the ESR line-width and the intensity of the signal.

Since in our first crystal structure determination of (BEDO-TTF)<sub>2</sub>ReO<sub>4</sub>·(H<sub>2</sub>O) [8, 12] a slight disorder in the ReO<sub>4</sub><sup>-</sup>-anions was indicated (probably due to a very slight twinning of the crystal), which was not observed later in the investigations of Buravov et al. [9], we have reinvestigated again the structure with a more perfect single crystal of (BEDO-TTF)<sub>2</sub>ReO<sub>4</sub>·(H<sub>2</sub>O). In this new refinement ( $R_w=0.040$ ) no disorder in the ReO<sub>4</sub><sup>-</sup>-anions was found in accordance with [9].

## Results

At room temperature for crystals of (BEDO-TTF)<sub>2</sub>ReO<sub>4</sub>·(H<sub>2</sub>O) the resistivity ratio  $\rho_c:\rho_{a^*}:\rho_b \approx 1:3:1000$  [10, 11]. This indicates that the electronic properties of the (BEDO-TTF)<sub>2</sub>ReO<sub>4</sub>·(H<sub>2</sub>O) crystals are less ideal two dimensional than those in radical salts of BEDT-TTF. In order to understand the electronic properties better several additional investigations were carried out. Figure 1 shows the resistivity ratio  $\rho_{a^*}:\rho_c$  for crystals of (BEDO-TTF)<sub>2</sub>ReO<sub>4</sub>·(H<sub>2</sub>O) in the temperature range 2 K to 300 K. It is interesting to notice that this ratio increases slowly by cooling the crystal but starts to increase more rapidly at about 90 K, the temperature where the thermopower measurements [8] indicate another phase transition. The ratio reaches its maximum value of ~6 at about 70 K. The maximum value at 70 K varies somewhat from crystal to crystal and was only ~4 for two other crystals. Below 70 K the ratio decreases to a value of 2. In the temperature range 50 K to 2 K the ratio is more or less constant, and especially in the temperature range below 35 K it does not change. The insert in Fig. 1 shows the resistivity  $\rho_c$  versus temperature.

Figure 2 shows the temperature dependence of the Hall resistivity  $R_H=I_c/U_H$ , where  $I_c$  is the current through the (BEDO-TTF)<sub>2</sub>ReO<sub>4</sub>·(H<sub>2</sub>O) crystal in *c*-direction, and  $U_H$  is the Hall voltage in *a*\*-direction (the magnetic field of 6.8 T is applied parallel to the *b*-direction). Over the whole temperature range of 1.5 K to 300 K the Hall voltage  $U_H$  is positive, indicating that the dominant contributing carriers are holes. Nevertheless, if it is assumed that the observed Hall voltage  $U_H$  at room temperature is due only to one type of carriers (holes), one obtains a carrier concentration 3 times larger than that expected from the stoichiometry of the crystals. This fact indicates that the observed Hall volt-

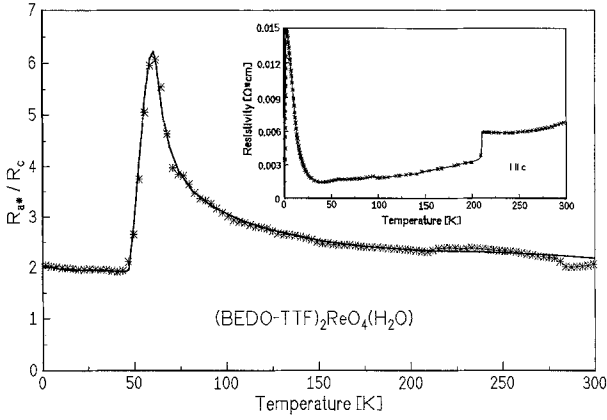


**Fig. 1.** Temperature dependence of the resistivity ratio  $\rho_{a^*}:\rho_c$  for crystals of  $(\text{BEDO-TTF})_2\text{ReO}_4 \cdot (\text{H}_2\text{O})$ . The insert shows the resistivity  $\rho_c$  versus temperature

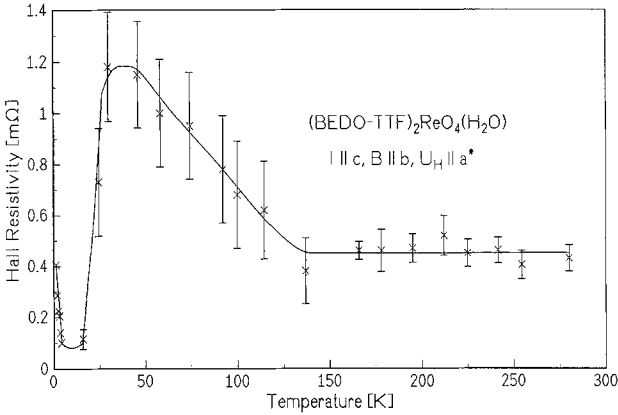
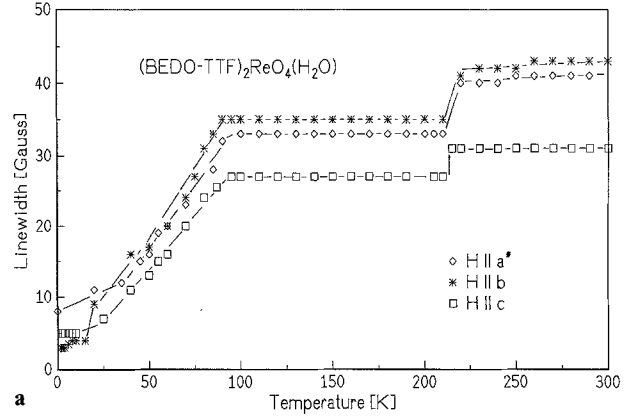


**Fig. 2.** Temperature dependence of the Hall resistivity  $R_H$  for  $(\text{BEDO-TTF})_2\text{ReO}_4 \cdot (\text{H}_2\text{O})$  (see text)

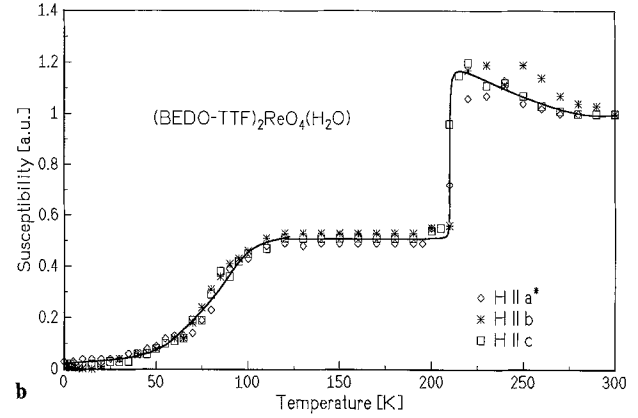
age originates from both hole and electron carriers. It should be noticed that within the experimental error there is no change in  $R_H$  at the phase transition of 213 K. On the other hand  $R_H$  decreases in the temperature range between 35 K and 10 K by a factor of ten.

Figure 3a plots the temperature dependence of the ESR linewidth of  $(\text{BEDO-TTF})_2\text{ReO}_4 \cdot (\text{H}_2\text{O})$  for the magnetic field parallel to the  $a^*$ -,  $b$ - and  $c$ -direction of the single crystals. Figure 3b shows an overview of the spin susceptibility derived from the ESR linewidth and the ESR signal amplitude. The phase transition at 213 K can be seen clearly in the temperature dependence of the ESR linewidth and the spin susceptibility. At the phase transition at 213 K, the spin susceptibility decreases abruptly by a factor of two. Below 100 K the ESR linewidth and the spin susceptibility start to decrease continuously, and the susceptibility at low temperatures is about 20 times smaller than the value at room temperature.

Figure 4 shows the magnetoresistance behavior of a  $(\text{BEDO-TTF})_2\text{ReO}_4 \cdot (\text{H}_2\text{O})$  crystal in the range 6 T to 24 T for several different temperatures between 0.5 K and 4.2 K (with the magnetic field  $B$  arranged perpendicular to the conducting plane and to the current flow



**a**



**b**

**Fig. 3. a** ESR linewidth of  $(\text{BEDO-TTF})_2\text{ReO}_4 \cdot (\text{H}_2\text{O})$  versus temperature for the magnetic field parallel to the  $a^*$ -,  $b$ - and  $c$ -direction. **b** Temperature dependence of the spin susceptibility of  $(\text{BEDO-TTF})_2\text{ReO}_4 \cdot (\text{H}_2\text{O})$  derived from the ESR line-width and intensity for the magnetic field parallel to the  $a^*$ -,  $b$ - and  $c$ -direction

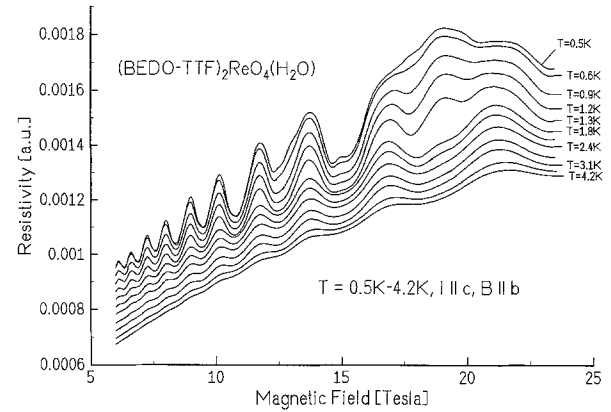


**Fig. 4.** Magnetoresistance (see text) of a single crystal of  $(\text{BEDO-TTF})_2\text{ReO}_4 \cdot (\text{H}_2\text{O})$  for several different temperatures

$I$ , which means  $B \parallel b$ -axis and  $I \parallel c$ -axis). SdH oscillations can clearly be seen at all temperatures below 4.2 K and at low temperatures the oscillation amplitude at high magnetic fields is about 30% of the nonoscillating part of the resistivity.

Figure 5a shows the SdH oscillations for another crystal of  $(\text{BEDO-TTF})_2\text{ReO}_4 \cdot (\text{H}_2\text{O})$  at 0.5 K versus the

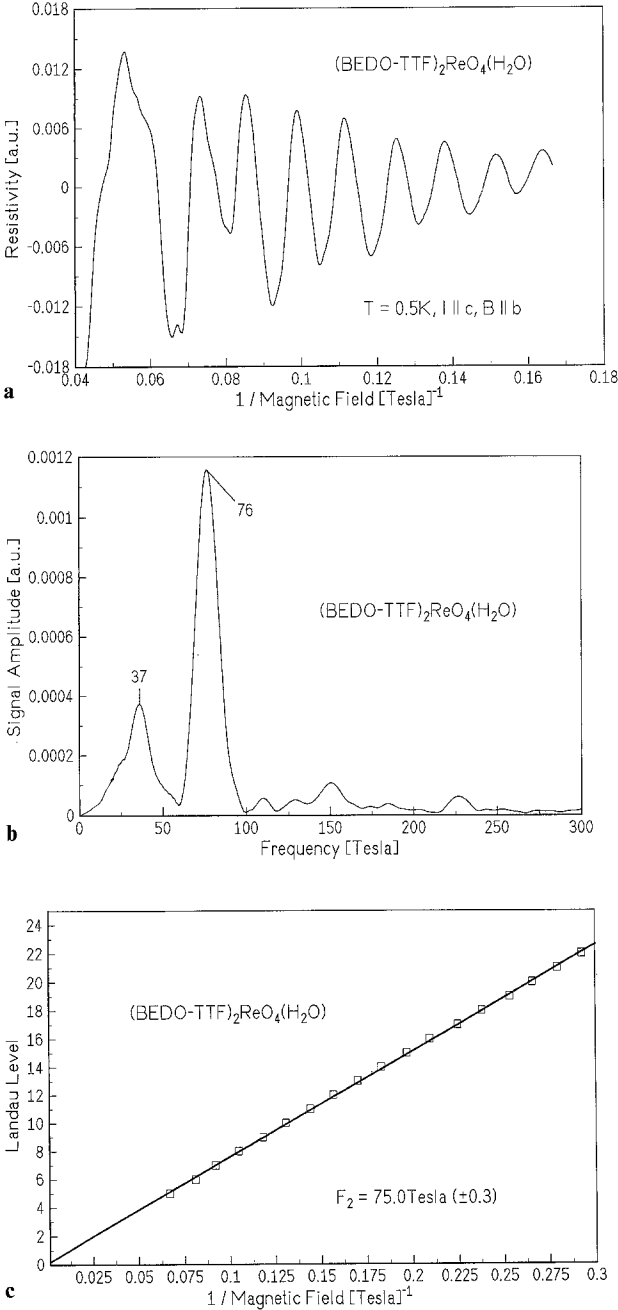


**Fig.5.** **a** SdH oscillations observed at 0.5 K for a single crystal of  $(\text{BEDO-TTF})_2\text{ReO}_4 \cdot (\text{H}_2\text{O})$  versus the reciprocal magnetic field ( $1/B$ ) with  $B \parallel b$  (see also text). **b** Fast Fourier transform of the digitally stored oscillation data from **a** between 6 and 24 T. **c** Number of Landau levels versus reciprocal field  $1/B$ . The solid line is a linear fit yielding  $F_2(0) = 75.0\text{ T}$

reciprocal magnetic field (for the range 6 T to 24 T). Here the sample orientation is the same as in Fig. 4, but the nonoscillating part of the resistivity was subtracted. Figure 5b shows the Fourier analysis of the digitally stored oscillations, which reveals that there exist two fundamental frequencies  $F_1 = (37 \pm 3)\text{ T}$  and  $F_2 = (76 \pm 2)\text{ T}$ . The corresponding extremal cross section areas  $A = (2\pi e/\hbar)F$  of the Fermi surface are  $A_1 = 0.35\text{ nm}^{-2}$  and  $A_2 = 0.75\text{ nm}^{-2}$  representing two closed pockets of the size of about 0.7% and 1.5% of the cross section of the first

Brillouin zone (FBZ). A more precise value of the frequency  $F_2 = (75.0 \pm 0.3)\text{ T}$  was obtained by linear regression from a plot of the number of Landau levels versus the reciprocal magnetic field, as shown in Fig. 5c.

The fast Fourier transform amplitudes of the frequencies  $F_1$  and  $F_2$  of the SdH oscillations were measured for eleven different temperatures in the field region between 6 T and 24 T. The temperature dependence of the amplitude was fitted to the temperature damping factor  $R_T$  of the Lifshitz-Kosevich formula:

$$R_T = \frac{rz}{\sinh rz}, \quad \text{with } z = \lambda \frac{m_c}{m_0} \frac{T}{B},$$

where  $\lambda = 2\pi^2 m_0 k_B / e\hbar = 14.693\text{ T/K}$ ,  $m_c$  is the cyclotron effective mass,  $m_0$  is the free electron mass and  $r$  is the number of the SdH harmonic ( $r = 1$  for the fundamental). From the slope of the corresponding plot (see Fig. 6a), the cyclotron effective masses were calculated: for the larger orbit (corresponding to  $F_2$ )  $m_c = (0.90 \pm 0.05) m_0$ , and for the smaller orbit (corresponding to  $F_1$ )  $m_c = (1.15 \pm 0.1) m_0$ . The error of the effective mass of the smaller orbit is larger due to the fact that the amplitude of the oscillation frequency  $F_1$  is much smaller than that of  $F_2$ . The effective mass for the larger orbit calculated from the amplitude of  $F_2$  for a fixed magnetic field of

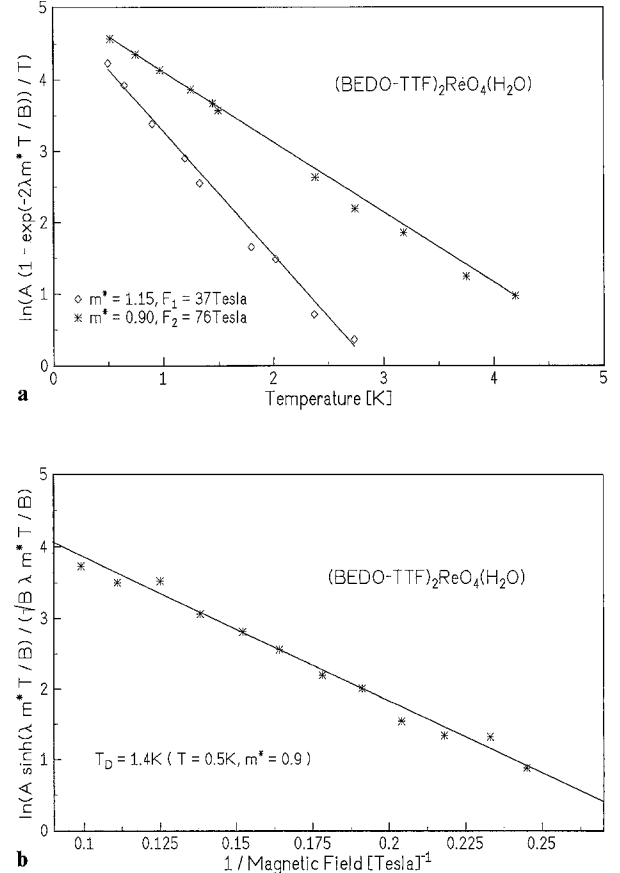


**Fig. 6.** **a** Temperature dependence of the SdH amplitudes of a  $(\text{BEDO-TTF})_2\text{ReO}_4 \cdot (\text{H}_2\text{O})$  crystal. **b** SdH amplitude versus inverse magnetic field  $1/B$ . The Dingle temperature was obtained from the slope of the straight line

13.5 T is  $0.9 m_0$ , which is in perfect agreement with the method described above.

With the value of the cyclotron mass known, the Dingle temperature  $T_D$  can be obtained from the magnetic field dependence of the oscillation amplitude, which is proportional to the Dingle damping factor  $R_D$  given by:

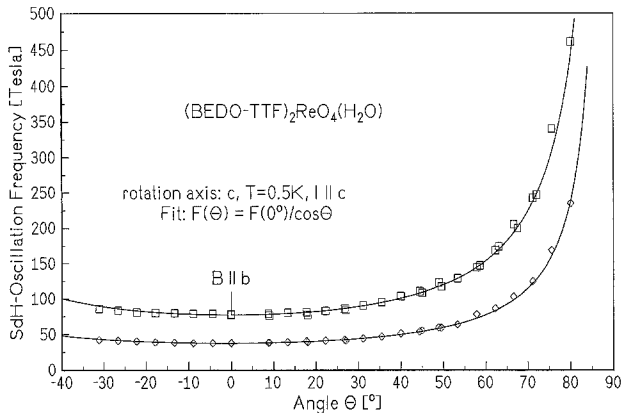
$$R_D = \exp\left(-r \lambda \frac{m_c}{m_0} \frac{T_D}{B}\right).$$

A fitting of the data for the frequency  $F_2$  (Fig. 6b) results in a Dingle temperature  $T_D = 1.4$  K. Considering  $T_D = \hbar/2\pi k_B \tau$ , the relaxation time is  $\tau \approx 0.9$  ps. In order to study the geometry of the Fermi surface in more detail, SdH measurements were carried out (beside the magnetic field  $B \parallel b$ ) for various angles of inclination  $\Theta$  between  $B$  and the  $b$ -axis. The SdH signal was observed in the field range 6 T to 24 T at 0.5 K. The  $F_1$  and  $F_2$  oscillations could be observed at angles up to  $80^\circ$ . Figure 7 shows the measured angular dependence of the SdH frequencies  $F_1$  and  $F_2$  for  $B \perp c$ . The data for both frequencies perfectly follow the behavior  $F(\Theta) = F(0)/\cos \Theta$ , shown by the solid line, as expected for a cylindrical Fermi surface of a quasi two dimensional organic metal.

## Electronic band structure

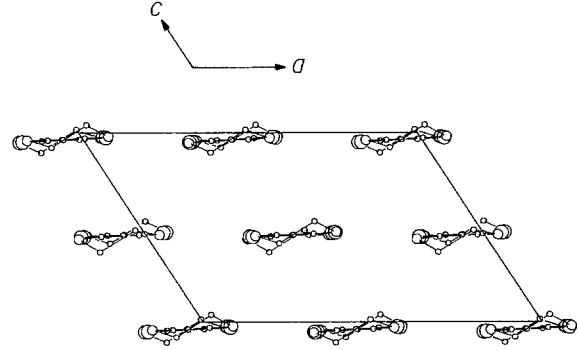
In the two crystal structures of  $(\text{BEDO-TTF})_2\text{ReO}_4 \cdot (\text{H}_2\text{O})$  reported in [8, 9] the employed crystallographic axis systems are different. In [8, 12] the donor molecule layer lies in the  $ac$ -plane and the  $a$ ,  $b$  and  $c$  axes correspond to the  $-a'$ ,  $c'$  and  $(a' + b')$  axes of Buravov et al. [9] respectively. In the present EHTB calculations, we employed the new refined crystal structure and the crystal axis system as used in [8, 12].

Figure 8 shows a schematic projection view of the donor molecule layer, which is contained in the  $ac$ -plane, where the sulfur, oxygen and carbon atoms are represented by large, medium and small circles, respectively. The donor molecules BEDO-TTF are inclined with respect to the donor molecule plane such that each BEDO-TTF of Fig. 8 is viewed approximately along the direc-



**Fig. 7.** Angular dependence of the SdH frequencies  $F_1$  and  $F_2$  for  $B \perp c$ . Solid lines: calculated curves for  $F(\Theta) = F(0)/\cos \Theta$

tion of its central  $\text{C}=\text{C}$  bond. The donor molecule layer consists of BEDO-TTF stacks running along the  $c$ -axis direction. A unit cell of the donor molecule layer contains two BEDO-TTF stacks, and that of each BEDO-TTF stack contains two BEDO-TTF molecules. We carried out EHTB calculations for a single donor molecule



**Fig. 8.** Perspective view of a donor molecule layer of  $(\text{BEDO-TTF})_2\text{ReO}_4 \cdot (\text{H}_2\text{O})$ . The large, medium and small circles represent the sulfur, oxygen and carbon atoms of BEDO-TTF, respectively, and the hydrogen atoms are not shown for simplicity. Each donor molecule is viewed roughly along the direction of its central  $\text{C}=\text{C}$  bond

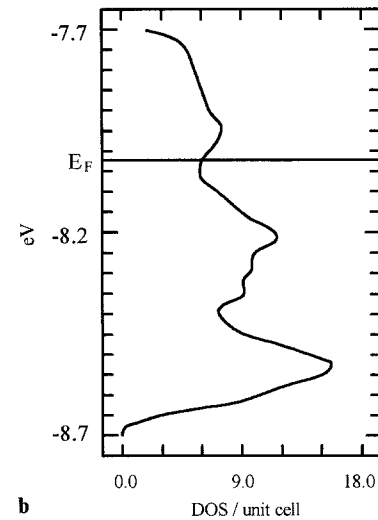
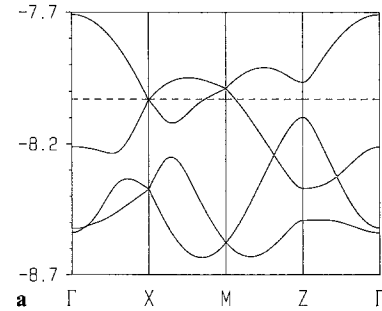


**Fig. 9.** **a** Dispersion relations of the four highest occupied bands calculated for a single donor molecule layer of  $(\text{BEDO-TTF})_2\text{ReO}_4 \cdot (\text{H}_2\text{O})$ , where the Fermi level is represented by the dashed line.  $\Gamma = (0, 0)$ ,  $X = (a^*/2, 0)$ ,  $M = (a^*/2, c^*/2)$ , and  $Z = (0, c^*/2)$ . **b** Density of states calculated for the four highest occupied bands of a single donor molecule layer of  $(\text{BEDO-TTF})_2\text{ReO}_4 \cdot (\text{H}_2\text{O})$

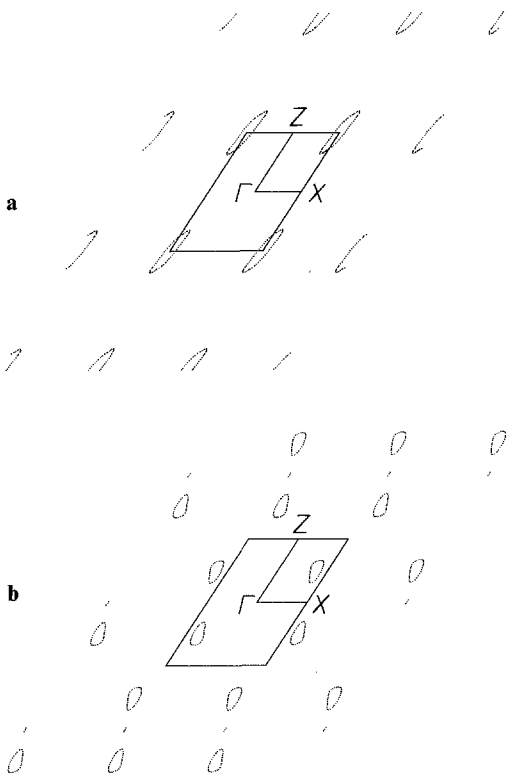


**Fig. 10.** Fermi surface of  $(\text{BEDO-TTF})_2\text{ReO}_4 \cdot (\text{H}_2\text{O})$  in an extended zone **a** hole pockets and **b** electron pockets.  $\Gamma = (0, 0)$ ,  $X = (a^*/2, 0)$ , and  $Z = (0, c^*/2)$

layer by employing the atomic parameters of the previous work [5].

Figure 9a shows the dispersion relation of the four highest occupied bands of  $(\text{BEDO-TTF})_2\text{ReO}_4 \cdot (\text{H}_2\text{O})$ , and Fig. 9b the density of states (DOS)  $n(e)$ , calculated for these bands. With the oxidation state  $(\text{BEDO-TTF})_2^+$ , there are six electrons to fill the four bands so that the highest two bands are partially filled. The Fermi surfaces associated with these bands are shown in Fig. 10. The hole surface (Fig. 10a) consists of a pocket centered at  $M$  with the size of  $\sim 3.4\%$  of the FBZ. The electron surface (Fig. 10b) consists essentially of two pockets with the size of  $\sim 1.7\%$  of the FBZ [another electron pocket occurs at  $X$ , but it is too small in size to be significant for the electronic properties of  $(\text{BEDO-TTF})_2\text{ReO}_4 \cdot (\text{H}_2\text{O})$ ]. Thus, our calculations predict that  $(\text{BEDO-TTF})_2\text{ReO}_4 \cdot (\text{H}_2\text{O})$  is a  $2D$  metal, in agreement with the experiment.

## Discussion

The most striking result of our investigations is the fact that the SdH measurements below 4.2 K show that  $(\text{BEDO-TTF})_2\text{ReO}_4 \cdot (\text{H}_2\text{O})$  has two kinds of closed Fermi surface pockets in excellent agreement with the Fermi surface calculated on the basis of the room temperature crystal structure. This is surprising in view of the fact that  $(\text{BEDO-TTF})_2\text{ReO}_4 \cdot (\text{H}_2\text{O})$  undergoes at least two (the thermopower [8] and the present Hall measure-

ments indicate even three) phase transitions by cooling the crystal down to 4.2 K. Therefore, we will now discuss in more detail the nature of the phase transitions at 213 K and around 35 K before we discuss the experimentally observed properties of the Fermi surface.

Let us first concentrate on the first order phase transition at 213 K. In the first report on  $(\text{BEDO-TTF})_2\text{ReO}_4 \cdot (\text{H}_2\text{O})$  [8] it was speculated that the 213 K metal metal transition is associated with anion ordering, because in this early investigations the structural data indicated a slight disorder in the  $\text{ReO}_4^-$  anions. Therefore, as in the case of  $(\text{TMTSF})_2\text{ReO}_4$  [21] at 180 K, it was assumed that at 213 K the ordering of the anions appears. Buravov et al. [9] showed later that the  $\text{ReO}_4^-$  anions are already ordered at room temperature, and they speculated that the transition at 213 K is caused by some reorientation of the  $\text{ReO}_4^-$  anions and/or  $\text{H}_2\text{O}$  molecules. Recent structural investigations at a temperature of 200 K on a crystal of  $(\text{BEDO-TTF})_2\text{ReO}_4 \cdot (\text{H}_2\text{O})$  [22] seem to indicate that a structural phase transition into a phase with lower symmetry (monoclinic-to-triclinic) occurs.

We now consider how the abrupt resistivity decrease at 213 K can be accounted for on the basis of the present electronic band structure calculations. To a first approximation, the resistivity  $\rho$  is inversely proportional to  $n(e_F)\tau$ , where  $n(e_F)$  is the density of states (DOS) at the Fermi level (i.e., the carrier density), and  $\tau$  the relaxation time. Thus, a decrease in  $\rho$  means an increase in  $\tau$  and/or  $n(e_F)$ . The present electronic band structure calculations show that  $(\text{BEDO-TTF})_2\text{ReO}_4 \cdot (\text{H}_2\text{O})$  is a semimetal, which arises from the fact that the top of the third band overlaps slightly with the bottom of the fourth band (see Fig. 9a). The extent of this band overlap might undergo a change to alter the  $n(e_F)$  value, if  $\text{ReO}_4^-$  anions and/or  $\text{H}_2\text{O}$  molecules reorient at the phase transition, because the latter will modify the intermolecular interactions between the BEDO-TTF molecules. Nevertheless, if the 213 K phase transition really induces a monoclinic-to-triclinic change [22], this change is expected to involve a slight tilting of the  $b$ -axis, which will leave unaffected the essential aspects of the electronic structure of the donor molecule layer. Otherwise, one cannot expect the low temperature physical properties of  $(\text{BEDO-TTF})_2\text{ReO}_4 \cdot (\text{H}_2\text{O})$  [as obtained by the SdH measurements] to be so well explained by the electronic band structure calculated on the basis of its room temperature crystal structure (see below). However, the DOS value  $n(e)$  does not vary abruptly around the Fermi level (see Fig. 9b) and indeed, the Hall effect measurements (see Fig. 2) suggest that the  $n(e_F)$  value remains constant during the 213 K phase transition since no change in the Hall resistivity is observed in this temperature range. (Since the Hall resistivity is composed of hole and electron contributions this argument is not rigorous because the concentration of both types of carriers could change in such a way that no change in the Hall resistivity is observed.) Then, the resistivity drop at 213 K would mean that the 213 K transition abruptly increases the relaxation time  $\tau$ . The latter is possible, because the lower temperature structure is likely to be more ordered.

On the other hand the ESR measurements on  $(\text{BEDO-TTF})_2\text{ReO}_4 \cdot (\text{H}_2\text{O})$  show that at the 213 K transition the spin susceptibility decreases by about a factor of two. Since the Pauli susceptibility is proportional to  $n(e_F)$ , the ESR data suggest that at the 213 K transition  $n(e_F)$  decreases by a factor of two. This seems to contradict the conclusion of the Hall effect measurements that the  $n(e_F)$  value remains constant during the 213 K transition. Nevertheless, the ESR and Hall effect measurements are in agreement in that the 213 K transition does *not* increase  $n(e_F)$ . Consequently, the resistivity drop at 213 K appears to be caused by an abrupt increase in the relaxation time  $\tau$ .

As for the phase transition at  $\sim 35$  K it was assumed in [8] that disorder phenomena in the anionic and/or cationic sublattice might drive this phase transition and therefore lead to the resistivity increase below 35 K. Buravov et al. [9] pointed out that this is unlikely since usually low temperature phases are more ordered. Furthermore microwave resistivity measurements [9] showed that the resistivity rise below 35 K at 10 GHz is much less pronounced, and thus they proposed by analogy with a similar observation in  $(\text{TMTSF})_2\text{PF}_6$  [23] that the  $\sim 35$  K transition is consistent with a phase transition into a charge density wave (CDW) or spin density wave (SDW) state, and further that an SDW state is more probable because the microwave frequency of 10 GHz is not large enough for the strong resistivity increase. In fact, our ESR measurements (see Fig. 3b) are consistent with this interpretation, because the susceptibility decreases very slowly in the region below 50 K. If the  $\sim 35$  K transition were a CDW, a sharp decrease of susceptibility would occur around  $\sim 35$  K. Actually the spin susceptibility starts to decrease already below 90 K, the temperature where the thermopower and Hall effect data indicate another phase transition, while above 90 K the spin susceptibility is constant as expected for a metallic system.

The proposal of an SDW state for the  $\sim 35$  K transition is in apparent contradiction to the calculated hole and electron Fermi surfaces (Fig. 10) because the latter, when viewed individually, do not possess any 1D character. We now examine a possible hidden nesting in  $(\text{BEDO-TTF})_2\text{ReO}_4 \cdot (\text{H}_2\text{O})$ . The hole and electron Fermi surfaces are combined together in Fig. 11a, which reveals that the hole and electron pockets form a set of ‘wavy patterns’ running along the  $c^*$ -direction. As depicted in Fig. 11b, each ‘wavy pattern’ of Fig. 11a may be considered to originate from a ‘wavy stripe’ weaving through the ‘outer’ boundaries of the hole and electron pockets. This is reasonable because, being essentially molecular crystals, organic salts have weak bonding between donor molecules and between molecules and anions. When the temperature is lowered, donor molecules may undergo slight local displacements to adjust to the ensuing decrease in the unit cell volume thereby changing the extend of the 1D or 2D character of the Fermi surface. The ‘wavy stripes’ of Fig. 11b are the hidden 1D surfaces associated with Fig. 11a, and their nesting can give rise to an electronic instability. The SDW instability as a cause for the  $\sim 35$  K transition

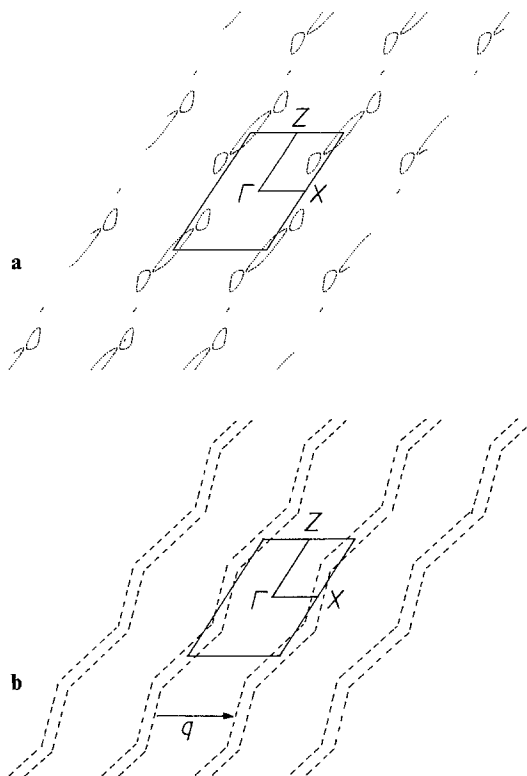


**Fig. 11.** **a** Hole and electron Fermi surface of  $(\text{BEDO-TTF})_2\text{ReO}_4 \cdot (\text{H}_2\text{O})$  combined together. **b** Hidden 1D Fermi surfaces associated with **a**.  $\Gamma = (0, 0)$ ,  $X = a^*/2, 0$ , and  $Z = 0, c^*/2$

is supported on the basis of the hidden nesting concept [15, 18]. The SDW formation removes some of the Fermi surfaces, which explains the finding from the Hall effect measurements (see Fig. 2) that there is a drastic change in the number of holes and electrons in the low temperature region.

As discussed in the previous section, why there occurs an SDW instability can be explained in terms of hidden nesting. However, the presence of hidden nesting does not necessarily mean that the system will be trapped in an SDW state. With decreasing temperature below 35 K, the system may gradually get out of the SDW state and re-enter the ‘original’ metallic state. This is not surprising because the nesting is not perfect to begin with. The situation is similar to the case of the crystals of  $(\text{TMTSF})_2\text{PF}_6$  under pressure [1], provided that the ‘internal pressure’ induced by lattice shrinking is sufficient for  $(\text{BEDO-TTF})_2\text{ReO}_4 \cdot (\text{H}_2\text{O})$ . This explains the presence of the closed Fermi surface pockets at temperatures below 5 K as observed by the SdH oscillations. In addition, this also explains the fact that a relatively low isotropic pressure of less than 1 kbar is sufficient to suppress the resistivity increase below 35 K [9–11] and sharpen the superconducting transition [10]. In the case of  $(\text{BEDO-TTF})_2\text{ReO}_4 \cdot (\text{H}_2\text{O})$  the ‘internal pressure’ induced by lattice shrinking might be sufficient to get out of the SDW state and to re-enter the ‘original’ metallic state, since the electronic properties of  $(\text{BEDO-TTF})_2\text{ReO}_4 \cdot (\text{H}_2\text{O})$  are certainly less anisotropic than those of the TMTSF radical salts, for which the

resistivity ratios along the three different directions are usually about 1:25:1000 [24].

In view of the calculated Fermi surface and the fact that over the entire temperature range between 1.3 K and 300 K in the magnetic field of 6.8 T the Hall effect is positive, we conclude that the closed pocket with about 1.5% (corresponding to the SdH oscillation frequency  $F_2$ ) of the size of the FBZ represents the hole pocket obtained by the EHTB calculation (see Fig. 10a), while the other pocket with about 0.7% ( $F_1$ ) of the size of the FBZ belongs to the electron pocket shown in Fig. 10b. The fact that the experimentally observed pockets have about half the size of the calculated ones is not surprising since the calculated Fermi surface was obtained from the room temperature structural data and the crystal undergoes at least two phase transitions by cooling down to 4.2 K. In fact we can conclude that the experimental results are in very good agreement with the EHTB calculations. In addition, the SdH data perfectly follow a  $F(\theta) = F(0)/\cos \theta$  behavior (see Fig. 7) as expected for a cylindrical Fermi surface of a quasi two dimensional metal. Furthermore it is now understandable that the calculated carrier concentration obtained from the Hall effect under the assumption that only one type of carriers exists is by far too large, since holes and electrons, both contribute to the Hall voltage.

In view of the small sizes of the closed pockets of only 1.5% and 0.7% of the FBZ, the observed cyclotron effective masses  $m_c$  ( $0.9 m_0$  and  $1.15 m_0$  respectively) are relatively large. Effective masses of carriers observed for such small pockets are usually much smaller [25]. Therefore, in the case of  $(\text{BEDO-TTF})_2\text{ReO}_4 \cdot (\text{H}_2\text{O})$  many-body interactions might give rise to an effective mass enhancement. To check whether this is true or not, further experiments are necessary.

## Conclusion

On the basis of electronic band structure calculations and SdH-, Hall effect- and ESR measurements, we investigated the probable causes for the 213 K and  $\sim 35$  K phase transitions in the organic superconductor  $(\text{BEDO-TTF})_2\text{ReO}_4 \cdot (\text{H}_2\text{O})$ . Our calculations show that  $(\text{BEDO-TTF})_2\text{ReO}_4 \cdot (\text{H}_2\text{O})$  is a 2D semimetal but possesses hidden 1D Fermi surfaces. The latter supports the proposal of an SDW instability for the  $\sim 35$  K transition. The resistivity drop at 213 K can be caused by an abrupt increase either in the relaxation time  $\tau$  or in the  $n(e_F)$  value. The former is likely to be correct according to both the Hall effect and ESR measurements. The SdH data show that  $(\text{BEDO-TTF})_2\text{ReO}_4 \cdot (\text{H}_2\text{O})$  has two kinds of closed surface pockets, in excellent agreement with the Fermi surface calculated on the basis of the room temperature crystal structure. Consequently, with decreasing temperature below  $\sim 35$  K,  $(\text{BEDO-TTF})_2\text{ReO}_4 \cdot (\text{H}_2\text{O})$  gradually must get out of the SDW state and re-enter the "original" metallic state. The characteristic  $1/\cos \theta$  behavior of the SdH oscillations shows that the Fermi surface has a perfect cylindrical shape as expected for such a layered structure. The relatively

large cyclotron effective masses observed for the hole and electron pockets indicate that many-body interactions might be important.

We gratefully acknowledge the use of the facilities of the High Magnetic Field Laboratory of the Max Planck Institut für Festkörperforschung in Grenoble. S.K. and D.S. would like to thank Drs. W. Biberacher (Garching), J. Wosnitza (Karlsruhe) and A.G.M. Jansen (Grenoble) for very stimulating discussions and assistance in the SdH measurements. This work was supported by the Forschungsschwerpunkt Supraleitung des Landes Baden-Württemberg and by the Commission of the European Communities [contract CI-CT 90-0863 [CD]]. Work at North Carolina State University was supported by the U.S. Department of Energy, Office of Basic Sciences, Division of Material Sciences, under Grant DE-FGO5-86ER45259. C.R. thanks Departament d'Ensenyament de la Generalitat de Catalunya (Catalonia, Spain) for Grant DOGC1551, which made it possible to visit North Carolina State University.

## References

1. Jerome, D., Mazaud, A., Ribault, M., Bechgaard, K.: J. Phys. (Paris) Lett. **41** L95 (1980)
2. For a recent review, see: Williams, J.M., Schultz, A.J., Geiser, U., Carlson, K.D., Kini, A.M., Wang, H.H., Kwok, W.K., Whangbo, M.-H., Schirber, J.E.: Science **252**, 1501 (1991)
3. Suzuki, T., Yamochi, H., Srdanov, G., Hinkelmann, K., Wudl, F.: J. Am. Chem. Soc. **111**, 3108 (1989)
4. Wudl, F., Yamochi, H., Suzuki, T., Isotalo, H., Fite, C., Kasmai, H., Liou, K., Srdanov, G., Coppens, P., Maly, K., Jensen, A.F.: J. Am. Chem. Soc. **112**, 2461 (1990)
5. Beno, M.A., Wang, H.H., Kini, A.M., Carlson, K.D., Geiser, U., Kwok, W.K., Thompson, J.E., Williams, J.M., Ren, J., Whangbo, M.-H.: Inorg. Chem. **29**, 1599 (1990)
6. Beno, M.A., Wang, H.H., Carlson, K.D., Kini, A.M., Frankenhach, G.M., Ferraro, J.R., Larson, N., McCabe, G.D., Thompson, J.E., Purnama, C., Vashon, M., Williams, J.M., Jung, D., Whangbo, M.-H.: Mol. Cryst Liq. Cryst. **181**, 145 (1990)
7. Wudl, F., Yamochi, H., Suzuki, T., Isotalo, H., Fite, C., Liou, K., Kasmai, H., Srdanov, G.: The physics and chemistry of organic superconductors, p. 358. Saito, G., Kagoshima, S. (eds). Berlin, Heidelberg, New York: Springer 1990
8. Kahlich, S., Schweitzer, D., Heinen, I., Song En Lan, Nuber, B., Keller, H.J., Winzer, K., Helberg, H.W.: Solid State Commun. **80**, 191 (1991)
9. Buravov, L.I., Khomenko, A.G., Kushch, N.D., Laukhin, V.N., Shegolev, A.I., Yagubskii, E.B., Rozenberg, L.P., Shibaeva, R.P.: J. Phys. I (France) **2**, 529 (1992)
10. Kahlich, S., Schweitzer, D., Auban Senzier, P., Jerome, D., Keller, H.J.: Solid State Commun. **83**, 77 (1992)
11. Kahlich, S., Schweitzer, D., Auban Senzier, P., Jerome, D., Keller, H.J.: Synth. Met. **56**, 2483 (1993)
12. Schweitzer, D., Kahlich, S., Heinen, I., Song En Lan, Nuber, B., Keller, H.J., Winzer, K., Helberg, H.W.: Synth. Meth. **56**, 2827 (1993)
13. Lomer, W.M.: Proc. Phys. Soc. (London) **80**, 489 (1962); Overhauser, A.W.: Phys. Rev. **128**, 1437 (1962)
14. Wilson, J.A., DiSalvo, F.J., Mahajan, S.: Adv. Phys. **24**, 117 (1975); DiSalvo, F.J.: Electron phonon interactions and phase transitions, p. 107. New York: Plenum Press 1977
15. Whangbo, M.-H., Canadell, E., Foury, P., Pouget, J.P.: Science **252**, 96 (1991); Canadell, E., Whangbo, M.-H.: Chem. Rev. **91**, 965 (1991); Whangbo, M.-H., Canadell, E.: J. Am. Chem. Soc. **114**, 9587 (1992)
16. Parkin, S.S.P., Engler, E.M., Schumaker, R.R., Lagier, R., Lee, V.Y., Scott, J.C., Green, R.: Phys. Rev. Lett. **50**, 270 (1983); Whangbo, M.-H., Beno, M.A., Leung, P.C.W., Emge, T.J.,

- Wang, H.H., Williams, J.M.: *Solid State Commun.* **59**, 813 (1986)
17. Gärtner, S., Heinen, I., Schweitzer, D., Nuber, B., Keller, H.J.: *Synth. Met.* **31**, 199 (1989)
18. Whangbo, M.-H., Ren, J., Liang, W., Canadell, E., Pouget, J.P., Ravy, S., Williams, J.M., Beno, M.A.: *Inorg. Chem.* **31**, 4169 (1992); Martin, J.D., Doublet, M.L., Canadell, E.: (to be published)
19. Whangbo, M.-H., Hoffmann, R.: *J. Am. Chem. Soc.* **100**, 6093 (1978)
20. Schweitzer, D., Polychroniadis, K., Klutz, T., Keller, H.J., Henning, I., Heinen, I., Haerberlen, U., Gogu, E., Gärtner, S.: *Synth. Met.* **27**, 465 (1988)
21. Parking, S.S.P., Jerome, D., Bechgaard, K.: *Mol. Cryst. Liq. Cryst.* **79**, 213 (1982)
22. Boubekeur, K.: Private communication
23. Buravov, L.I., Laukhin, V.N., Khomenkov, A.G.: *Sov. Phys. JETP* **61/6**, 1292 (1985)
24. Green, R.L., Haen, P., Huang, S.Z., Engler, E.M., Choi, M.Y., Chaikin, P.M.: *Mol. Cryst. Liq. Cryst.* **79**, 183 (1982)
25. Shoenberg, D.: *Magnetic oscillations in metals*. Cambridge: Cambridge University Press 1984